Supplementary Information

Investigation of the tendency of carbon fibers to disintegrate into respirable fiber-shaped fragments

Asmus Meyer-Plath [1,*], Dominic Kehren [1], Anna Große [2], Romy Naumann [2], Marcel Hofmann [2], Tanja Schneck [3], Antje Ota [3], Frank Hermanutz [3], Nico Dziurowitz [1], Carmen Thim [1], Sabine Plitzko [1] and Daphne Bäger [1]

1 Federal Institute for Occupational Safety and Health (BAuA), 10317 Berlin, Germany; dominic.kehren@vdivde-it.de (D.K.); dziurowitz.nico@baua.bund.de (N.D.); thim.carmen@baua.bund.de (C.T.); s.plitzko@gmx.net (S.P.); baeger.daphne@baua.bund.de (D.B.)
2 Sächsisches Textilforschungsinstitut e.V. (STFI), 09125 Chemnitz, Germany; romy.naumann@stfi.de (R.N.)
3 German Institutes of Textile and Fiber Research Denkendorf (DITF), 73770 Denkendorf, Germany; frank.hermanutz@ditf.de (F.H.)
* Correspondence: meyer.plath.asmus@baua.bund.de

1 Measurements of the material properties

1.1 Counting rules

The filter samples generated by means of the described method for spallation characterization were imaged by a SEM (type SU8230, Hitachi High-Technologies Europe GmbH, Krefeld, Germany). The following counting rules were used for the evaluation of the acquired SEM images and thus to characterise the grinding material obtained:

SEM-imaging

About 25 randomly distributed filter locations are imaged with a size of 5120x3840 pixels, an electron beam energy of 2 keV and a working distance of 8 mm. Two images are acquired at each filter position

- One image with a magnification of 800x, corresponding to a pixel resolution of $\Delta P_{800\mathrm{x}} = 31$ nm
- One image with a magnification of 400x, corresponding to a pixel resolution of $\Delta P_{400\mathrm{x}} = 62$ nm

Evaluation of SEM images

The images of $\Delta P_{800\mathrm{x}} = 31$ nm are evaluated.

- At least 500 objects are counted.
- Complete images are counted until the count limit of 500 is reached. If the limit is reached, the current picture is counted until finished.
- The counting has to be done for a minimum of 5 images. If the limit of 500 objects is reached with fewer images, the counting has to be continued until 5 images are completed.
- During the evaluation, a zoom level has to be chosen that enables to easily identify objects of 1 µm in diameter.

Every fragment with an aspect ratio of 3:1 or higher, based on the mean diameter, counts as fibrous. Fibrous fragments are counted and measured (length, width).

- Only fibrous fragments are counted that:
  - are lying isolated,
  - whose beginning and end are in the image frame (exception: fibres with original diameter see below),
  - whose beginning and end can be clearly identified (not heavily covered by other fragments),
  - are in contact with other fibres or particles or form a fibre bundle or pile, but have clearly recognizable boundaries (Figure S1.1).
- Fibre bundles or particle agglomerates in which the objects cannot be clearly distinguished from one another, but which collectively have an aspect ratio greater than 3, are counted as one fibre and identified as a fibrous agglomerate (Figure S1.2).
- Fibres that lie on significantly larger fibres or particles, that are not isolated, are not counted separately (Figure S1.3).
- Fibres with approximately the original diameter (manufacturer information) or larger are categorized as original fibres and recorded separately in order to later calculate their added lengths.

  - If such a fibre protrudes from the image, the image of $\Delta P_{400x} = 62$ nm is used to determine the entire length of the fibre (Figure S1.4).
  - These fibres are marked as OF
- All fibres are categorized as HARFO (high aspect ratio fibre object) or HARFA (high aspect ratio fibre agglomerate)

In addition, all non-fibrous fragments (AR<3) are counted, but not measured exactly.

- Particles with approximately the original diameter or larger are marked as OP.
- All particles are categorized as LARPO (low aspect ratio particle object)
- Particles that lie on much larger fibres or particles, that are not isolated, are not counted separately (Figure S1.3).
- Particle agglomerates in which the particles cannot be clearly distinguished from one another are counted as one particle (Figure S1.2).

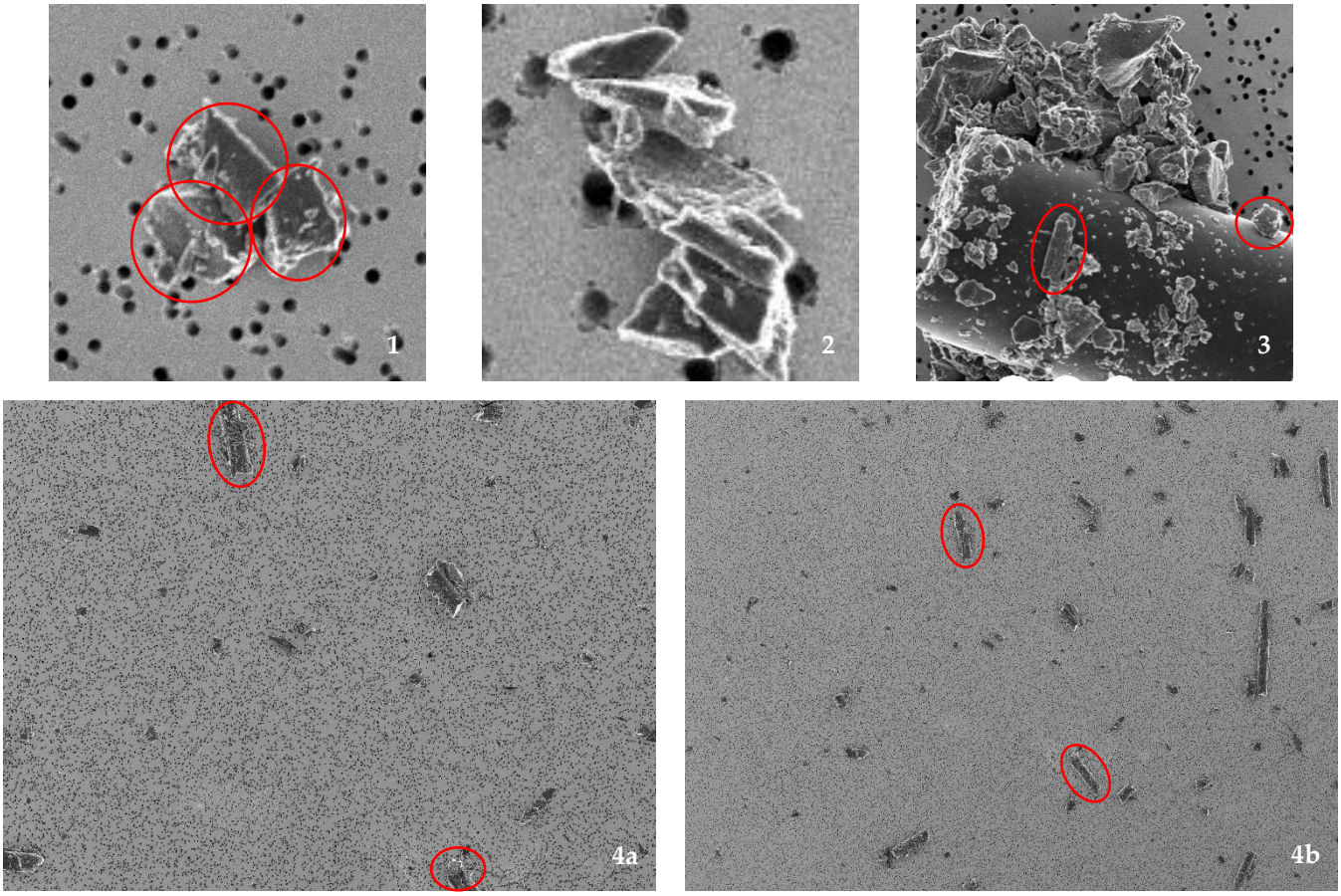

Figure S1: Examples of SEM images with different fragments: (1) particle cluster that can be counted as 3 individual particles because of recognizable boundaries, (2) particle cluster with unclear delimitations that is counted as one particle, (3) overlying particles or fibres that are not counted, (4) original fibres (OF) at the frame of the SEM image of $\Delta P_{800x} = 31$ nm (a) and their dimensions in the image of $\Delta P_{400x} = 62$ nm (b).

1.2 Estimation of missing thermal volume conductivity data

Thermal volume conductivity is generally not a key property for applications of panCF and values are specified by the manufacturers only for pitchCF. Since, we had no possibility to measure it, some thermal conductivity values were missing. However, a high linear correlation between the electrical volume conductivity q_E and the thermal volume conductivity q_T allowed to interpolate missing thermal values for panCF 5, 8 and 15 from the known values of the other CF using the formula $q_T = (q_E \cdot 1284.8\ \mathrm{W \cdot \mu\Omega/K} - 58.2\ \mathrm{W/m/K})$ that exhibited a Pearson correlation coefficient of 0.999, see Fig. S2.

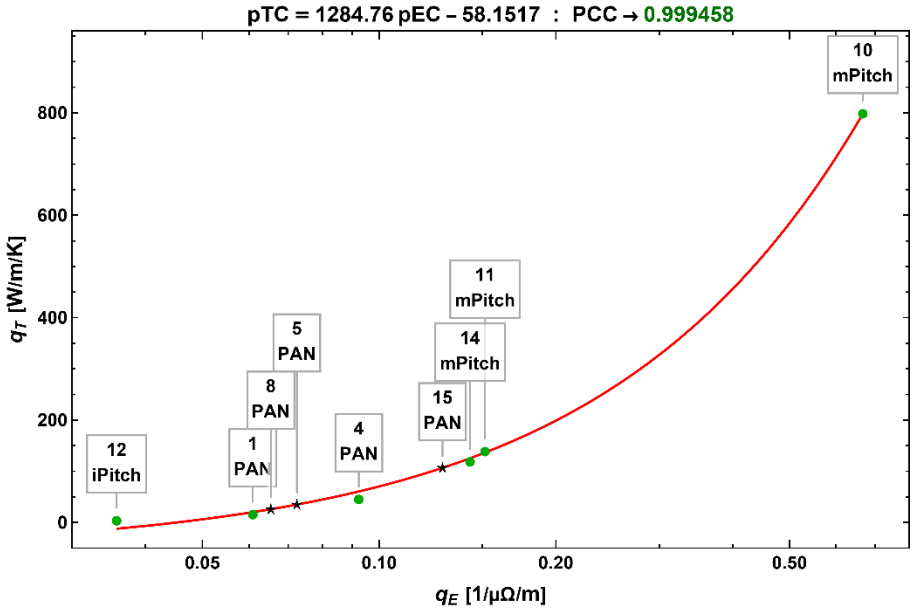

Figure S2: Log-linear plot of the linear interpolation of the known values of thermal and electrical volume conductivity (green dots and red line) to estimate the unknown thermal volume conductivities of CF materials 5, 8 and 15 (black stars).

1.3 Interpretation of Raman spectra

Raman measurements were performed with a WITec Apyron 300RA confocal Raman microscope (WITec GmbH, Ulm, Germany) equipped with a spectrometer of 300 mm focal length (UHTS 300), a 600 lines/mm grating and an EMCCD camera using 0.5 mW laser power at 532 nm. The area ratio of the G- and D-bands $A_{\mathrm{BWF}}(G)/A(D)$ were determined by fitting the spectra with a superposition of an offset value with 7 Lorentzian and, for the G band, a Breit-Wigner-line, see article.

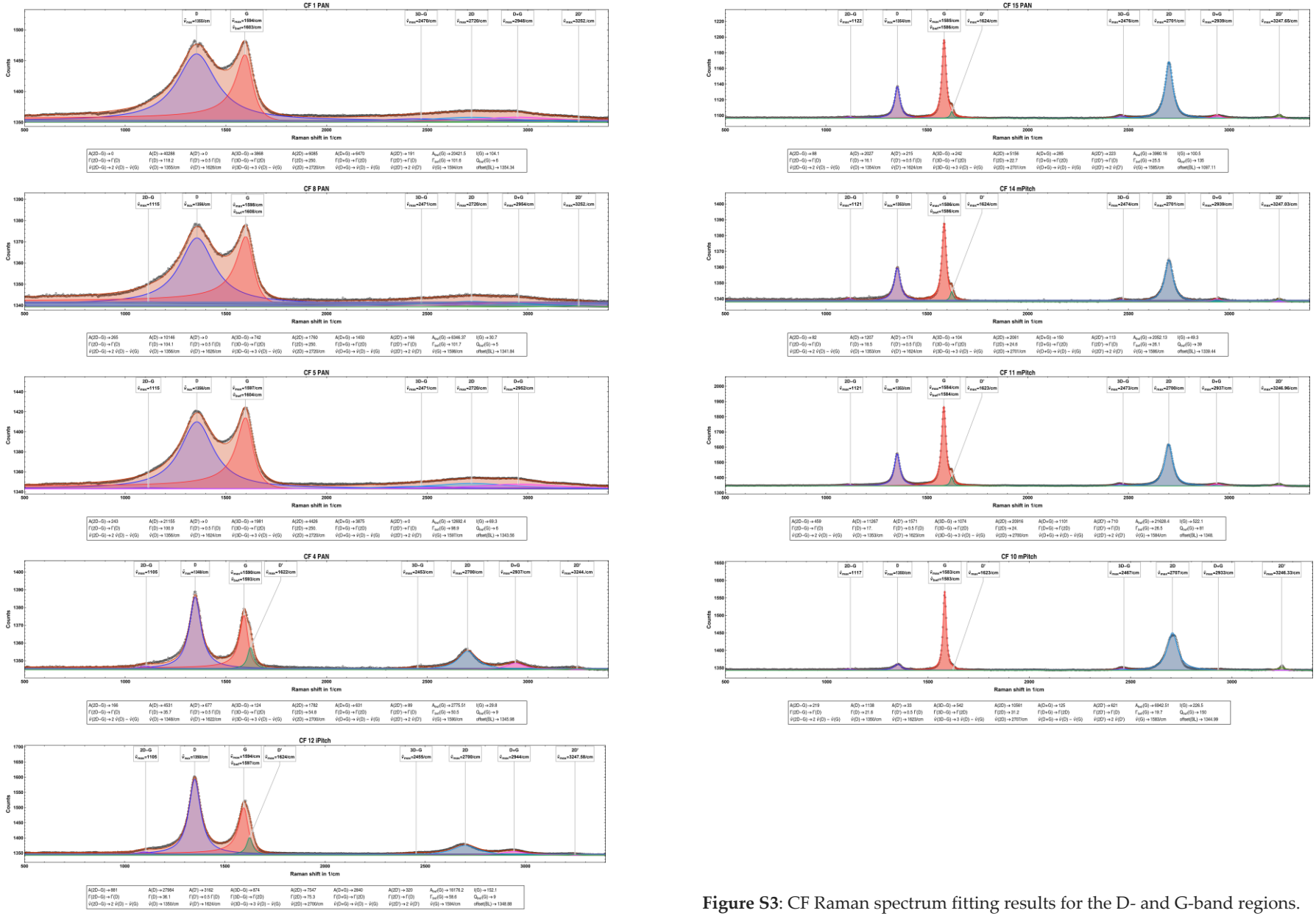

Figure S3: CF Raman spectrum fitting results for the D- and G-band regions.

1.4 Fracture morphology after ball milling

In Figures S4 to S6 the dataset underlying Table 5 of the manuscript was grouped in the following morphological classes: WHOFOs, HARFCs, i.e. HARFOs of about initial diameter, HARFSs, i.e. HARFOs thinner than the initial diameter, and HARFOs too thick or too short to be a WHOFO. For relative diameters, the vertical error bars do not include the uncertainty on the initial diameter.

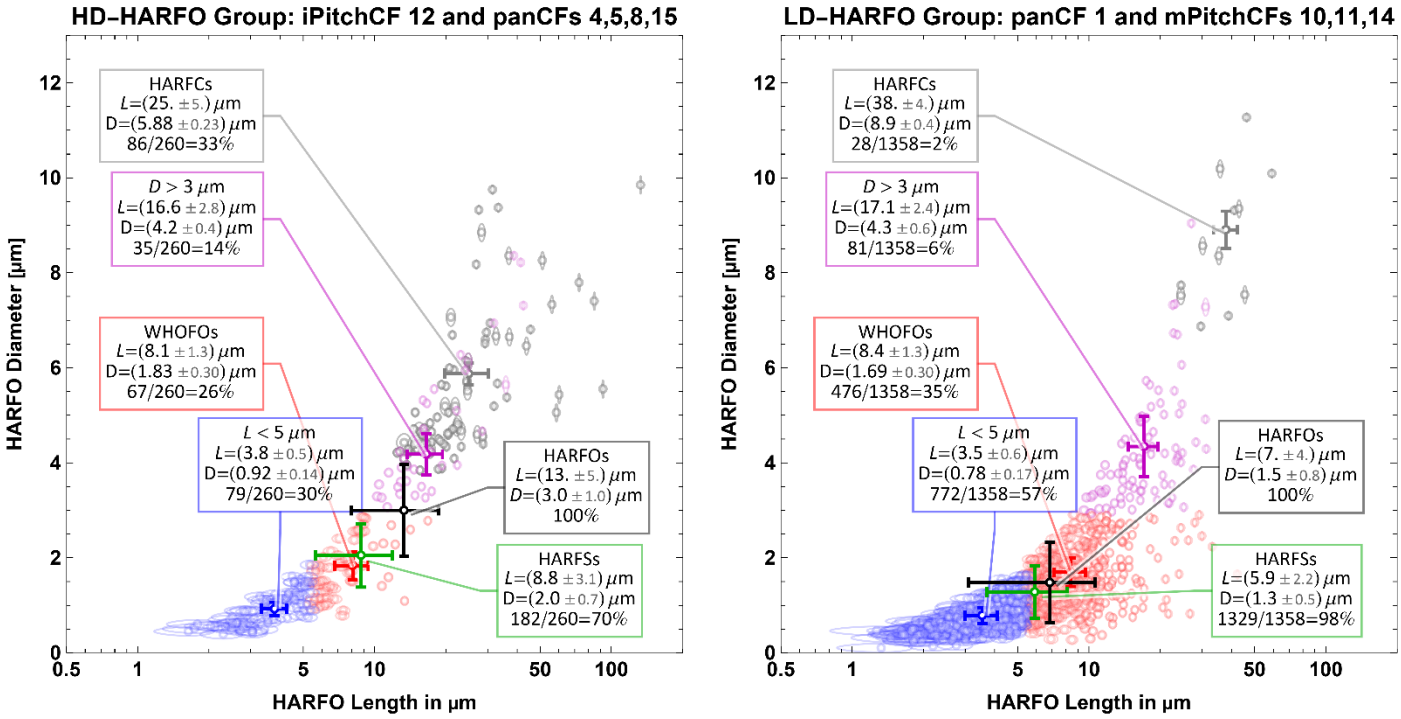

Figure S4: Same data as in Figure 4 of the publication but now for absolute HARFO diameters D versus the associated HARFO lengths L.

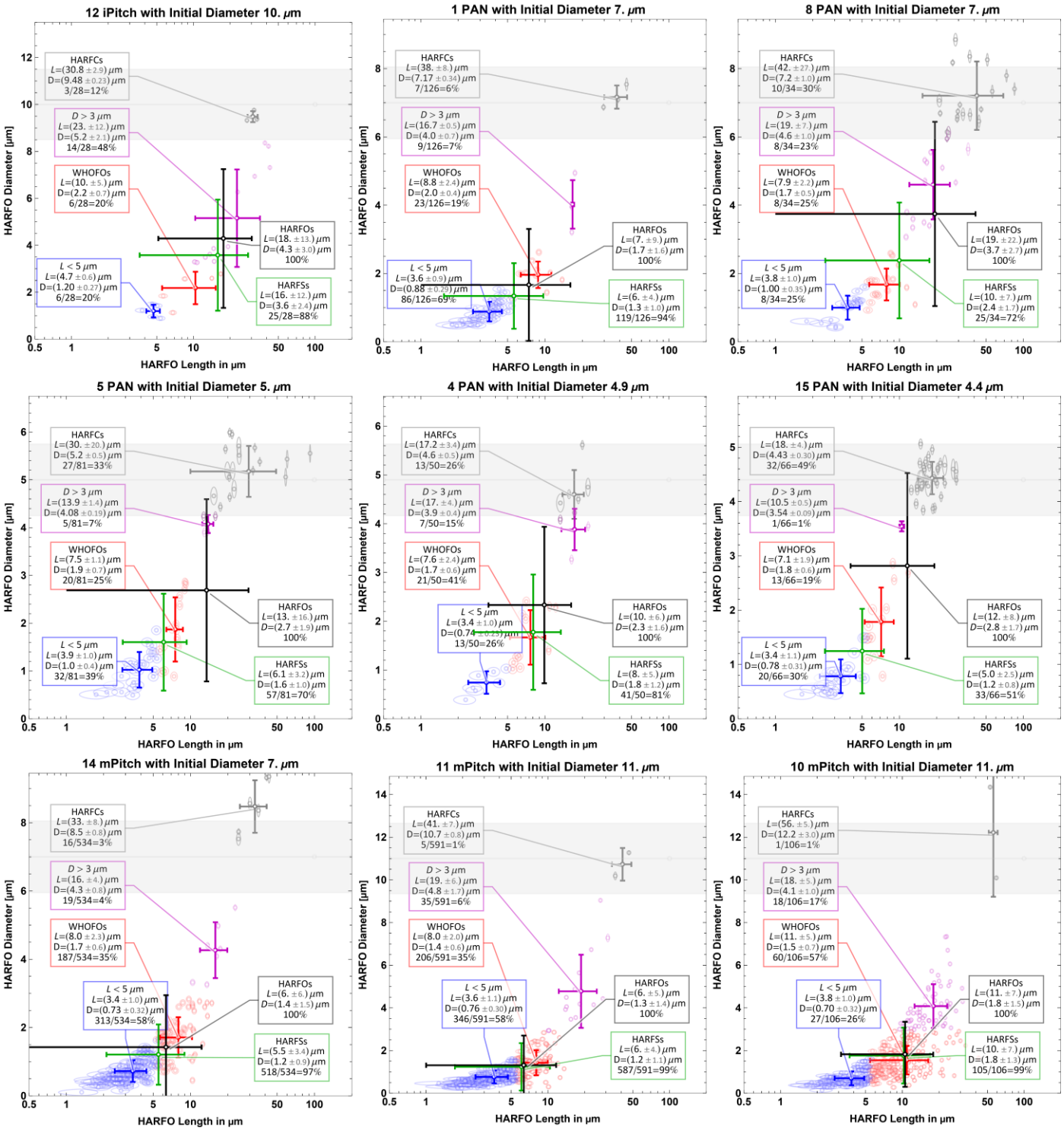

Figure S5: Distribution of the HARFO diameters D, normalized to the initial CF diameter d_i, versus the associated HARFO length L differentiated by the morphological subclass. HARFCs are shown in grey, HARFOs too short or too thick to be a WHOFO are shown in blue and purple, respectively, whereas WHOFOs are shown in red. The labels give averaged diameter and length as well as subclass count n relative to all N HARFO fragments. The average of all HARFS and HARFO subclasses is marked by a green and black error cross, respectively. The grey band marks the assumed relative error of 15% on the initial CF diameter. The HARFO counts obtained for a specific mass and filter area were renormalized here to the average 0.321 mm² evaluated area and 0.055 mg ground CF mass on a filter of 25 mm diameter with, therefore the number of displayed markers does not necessarily match the fragment count used for calculating observable averages.

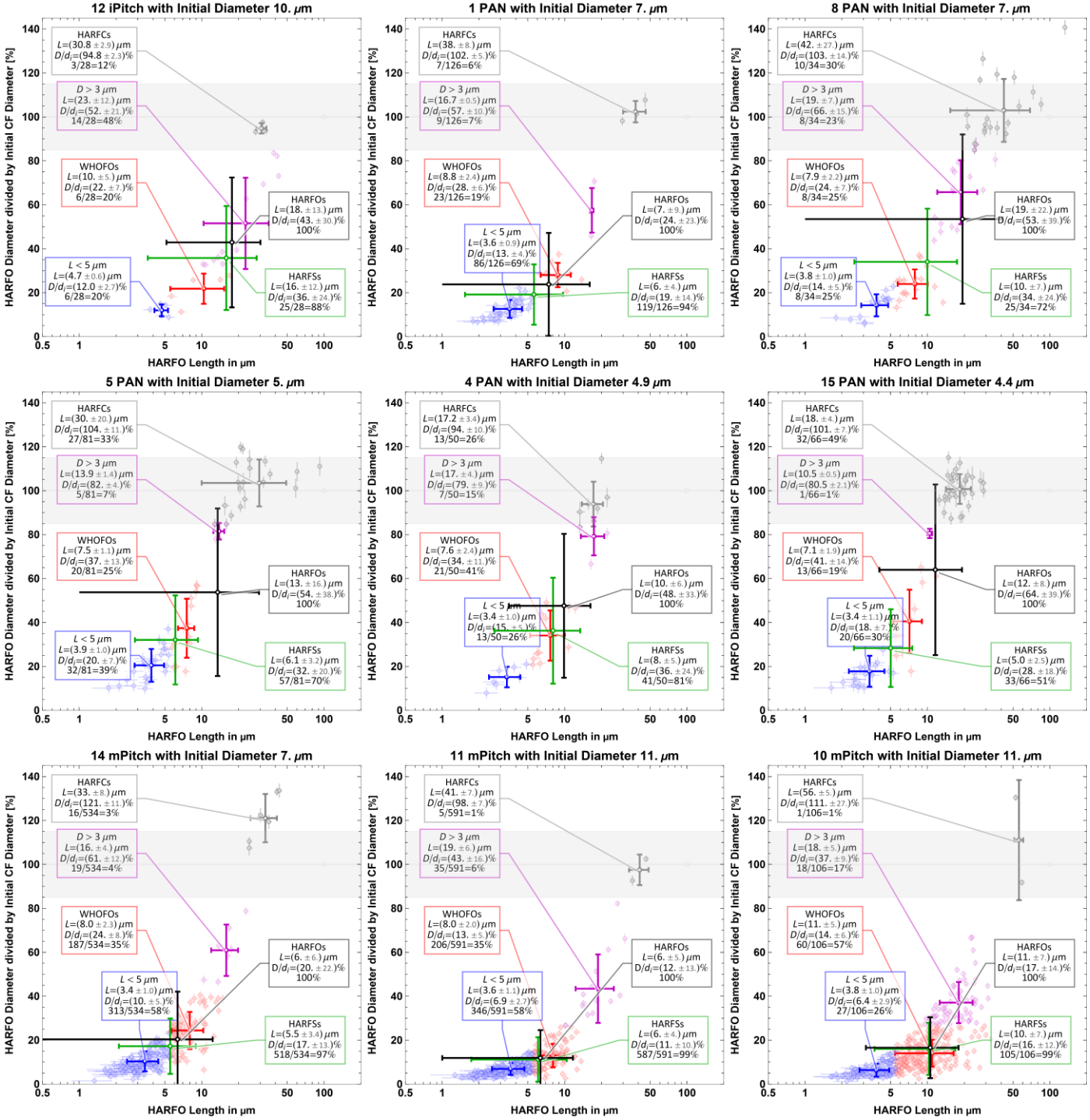

Figure S6: Same data as in Figure S3 but now for absolute HARFO diameters D versus the associated HARFO lengths L.

2 Applied error model

The applied model for error-weighted χ^2-fitting and diagram plotting is tabulated in Tab. S1.

Table S1: Applied error model for properties and observables as used for error-weighted χ^2-testing.

Name	Symbol	Assumed Error
Microporosity P_μ Percentage	pμP	$(1 - 0.15\ \mathrm{g/cm^3} \cdot 0.003\ \mathrm{nm}/0.335\ \mathrm{nm})$
Density ϱ	pϱ	$0.15\ \mathrm{g/cm^3}$
Partial Orientation O_P Percentage	pPO	5% pPO
d_{002}	pd002	0.003 nm
Tensile Modulus E_L	pTM	50 GPa + 5% pTM
Elongation at Break ε_B Percentage	pEaB	0.25%
Tensile Strength σ_T	pTS	250 MPa + 5% pTS
Initial Diameter d_i	pDI	1 μm
$L_{a\perp}$	pLaT	0.5 nm + 15% pLaT
$L_{a\parallel}$	pLaII	0.5 nm + 15% pLaII
Th.Conductivity q_T	pTC	15% pTC
Raman A_G/A_D	pRAGbyAD	$(1/\sqrt{\mathrm{iRAG}} + 1/\sqrt{\mathrm{iRAD}}) \cdot (\mathrm{iRAG}/\mathrm{iRAD})$
WHOFOs per Milled CF Volume	oWHOFOpl	$(1/\sqrt{\mathrm{oWHOFOmg}} + 1/\sqrt{\mathrm{p}\varrho}) \cdot (\mathrm{oWHOFOmg}/\mathrm{p}\varrho)$
HARFOs per Milled CF Volume	oHARFOpl	$(1/\sqrt{\mathrm{oHARFOmg}} + 1/\sqrt{\mathrm{p}\varrho}) \cdot (\mathrm{oHARFOmg}/\mathrm{p}\varrho)$
Mean Length of WHOFOs	oLMWHOFO	Standard Deviation(oLMWHOFO)
Mean Length of HARFOs	oLMHARFO	Standard Deviation(oLMHARFO)
Mean Aspect Ratio of WHOFOs	oARMWHOFO	Standard Deviation(oARMWHOFO)
Mean Aspect Ratio of HARFOs	oARMHARFO	Standard Deviation(oARMHARFO)
Mean Diameter of WHOFOs	oDMWHOFO	Standard Deviation(oDMWHOFO)
Mean Diameter of HARFOs	oDMHARFO	Standard Deviation(oDMHARFO)
WHOFOs to HARFOs Percentage	oWHOFO2HARFO	$(1/\sqrt{\mathrm{iWHOFOcnt}} + 1/\sqrt{\mathrm{iHARFOcnt}}) \cdot (\mathrm{iWHOFOcnt}/\mathrm{iHARFOcnt})$
WHOFOs per Milled CF Mass	oWHOFOmg	$(1/\sqrt{\mathrm{iWHOFOpFA}} + 1/\sqrt{\mathrm{iFMass}}) \cdot (\mathrm{iWHOFOpFA}/\mathrm{iFMass})$
HARFOs per Milled CF Mass	oHARFOmg	$(1/\sqrt{\mathrm{iHARFOpFA}} + 1/\sqrt{\mathrm{iFMass}}) \cdot (\mathrm{iHARFOpFA}/\mathrm{iFMass})$
WHOFOs per Filter Area	iWHOFOpFA	$(1/\sqrt{\mathrm{iWHOFOcnt}} + 1/\sqrt{\mathrm{iFArea}}) \cdot (\mathrm{iWHOFOcnt}/\mathrm{iFArea})$
HARFOs per Filter Area	iHARFOpFA	$(1/\sqrt{\mathrm{iHARFOcnt}} + 1/\sqrt{\mathrm{iFArea}}) \cdot (\mathrm{iHARFOcnt}/\mathrm{iFArea})$
Mass on filter	iFMass	15% iFMass
Evaluated Filter Area	iFArea	15%iFArea
WHOFO count	iWHOFOcnt	$\sqrt{\mathrm{iWHOFOcnt}}$
HARFO count	iHARFOcnt	$\sqrt{\mathrm{iHARFOcnt}}$
Raman G BWF Peak Area	iRAG	$\sqrt{\mathrm{iRAG}}$
Raman D Lorentz Peak Area	iRAD	$\sqrt{\mathrm{iRAD}}$

3 Kolmogorov-Smirnov test

As reported in the main article, material parameters and observables were submitted to a Kolmogorov-Smirnov test to compare their distribution to that of a Normal distribution with the mean and the standard deviation of the dataset.

The following Table S2 presents the individual responsibility of the fibre types to cause a deviation from Normality. The p_{KS}-value of only eight of the nine CF materials was calculated after omitting one CF type. The relative change of the p_{KS}-value of eight CFs with respect to that of the nine is tabulated only for increasing p_{KS}-values. Such increase indicates that Normality assumption is more significant for the tested eight than the nine CFs. Omitting that specific material rendered the remaining eight materials more homogeneous with respect to ensemble Normality. For some properties and observables, omitting a panCF appears to balance the larger group of low temperature materials (12,1,8,5,4) to the smaller group of high temperature materials (15,14,11,10). To increase the ensemble's Normality, it is therefore more effective to remove one of the panCF. This does not necessarily imply that the panCF materials contain an outlier. In addition, changes to smaller absolute p_{KS}-values for the full ensemble cause larger relative effect.

Table S2: Analysis results on individual fibre type responsibilities for a deviation from Normality with respect to material parameters (**top**) and observables (**bottom**).

	p_{KS}–value										Increase of p_{KS}–value									Relative Increase of p_{KS}–value								
CF Material removed from KS–Test Ensemble	**None**	**12**	**1**	**8**	**5**	**4**	**15**	**14**	**11**	**10**	**12**	**1**	**8**	**5**	**4**	**15**	**14**	**11**	**10**	**12**	**1**	**8**	**5**	**4**	**15**	**14**	**11**	**10**
Mean	**0.66**	**0.72**	**0.78**	**0.80**	**0.75**	**0.68**	**0.63**	**0.68**	**0.63**	**0.63**	**0.07**	**0.12**	**0.14**	**0.11**	**0.06**	**0.02**	**0.04**	**0.00**	**0.01**	**15%**	**23%**	**28%**	**23%**	**15%**	**3%**	**6%**	**0%**	**1%**
Microporosity P_μ	0.43	0.47	0.60	0.68	0.67	0.68	0.27	0.39	0.40	0.41	0.04	0.17	0.24	0.24	0.24	–	–	–	–	10%	40%	57%	55%	56%	–	–	–	–
Density ϱ	0.47	0.49	0.71	0.71	0.71	0.59	0.31	0.43	0.43	0.45	0.02	0.24	0.24	0.24	0.11	–	–	–	–	5%	51%	51%	51%	24%	–	–	–	–
Partial Orientation O_P	0.69	0.72	0.73	0.82	0.80	0.72	0.65	0.64	0.63	0.60	0.03	0.04	0.13	0.11	0.03	–	–	–	–	5%	6%	19%	16%	5%	–	–	–	–
d_{002}	0.99	0.99	0.98	0.96	0.93	0.98	1.00	0.99	0.99	0.92	–	–	–	–	–	–	–	–	–	–	–	–	–	–	–	–	–	–
Tensile Modulus E_L	0.98	0.96	1.00	1.00	0.98	0.87	0.94	0.93	0.95	0.97	–	0.02	0.02	0.01	–	–	–	–	–	–	2%	2%	1%	–	–	–	–	–
Log($L_{a\perp}$)	0.69	0.85	0.93	0.90	0.88	0.58	0.61	0.65	0.65	0.61	0.15	0.24	0.21	0.19	–	–	–	–	–	22%	34%	30%	27%	–	–	–	–	–
Log($L_{a\|\|}$)	0.59	0.81	0.81	0.82	0.85	0.43	0.52	0.55	0.55	0.55	0.22	0.22	0.24	0.26	–	–	–	–	–	38%	38%	40%	45%	–	–	–	–	–
Log(Th.Conductivity q_T)	0.96	0.92	0.93	0.95	0.96	0.97	0.98	0.98	0.97	0.91	–	–	–	–	0.01	0.02	0.02	0.01	–	–	–	–	–	1%	2%	2%	1%	–
Log(Raman A_G/A_D)	0.30	0.50	0.45	0.49	0.51	0.52	0.24	0.23	0.24	0.22	0.20	0.15	0.19	0.21	0.22	–	–	–	–	65%	50%	63%	69%	71%	–	–	–	–
Elongation at Break ε_B	0.73	0.71	0.70	0.68	0.71	0.56	0.74	0.74	0.76	0.76	–	–	–	–	–	0.01	0.01	0.03	0.03	–	–	–	–	–	1%	1%	4%	4%
Tensile Strength σ_T	0.54	0.74	0.64	0.70	0.34	0.62	0.70	0.73	0.37	0.58	0.20	0.09	0.16	–	0.07	0.16	0.19	–	0.03	36%	17%	29%	–	14%	29%	34%	–	6%
Initial Diameter d_i	0.60	0.50	0.84	0.84	0.64	0.63	0.56	0.84	0.58	0.58	–	0.24	0.24	0.04	0.03	–	0.24	–	–	–	40%	40%	7%	5%	–	40%	–	–

	p_{KS}–value										Increase of p_{KS}–value									Relative Increase of p_{KS}–value								
CF Material removed from KS–Test Ensemble	**None**	**12**	**1**	**8**	**5**	**4**	**15**	**14**	**11**	**10**	**12**	**1**	**8**	**5**	**4**	**15**	**14**	**11**	**10**	**12**	**1**	**8**	**5**	**4**	**15**	**14**	**11**	**10**
Mean	**0.55**	**0.60**	**0.60**	**0.62**	**0.60**	**0.59**	**0.57**	**0.53**	**0.53**	**0.62**	**0.05**	**0.07**	**0.08**	**0.09**	**0.07**	**0.05**	**0.03**	**0.03**	**0.09**	**19%**	**25%**	**27%**	**30%**	**27%**	**21%**	**8%**	**8%**	**27%**
WHOFOs per Milled CF Volume [1/pL]	0.16	0.26	0.26	0.26	0.28	0.29	0.27	0.14	0.14	0.08	0.10	0.10	0.10	0.13	0.13	0.11	–	–	–	62%	66%	66%	80%	81%	72%	–	–	–
HARFOs per Milled CF Volume [1/pL]	0.10	0.13	0.17	0.14	0.16	0.14	0.15	0.09	0.11	0.16	0.04	0.08	0.04	0.06	0.05	0.05	–	0.02	0.06	38%	80%	41%	61%	48%	57%	–	18%	67%
Mean Length of WHOFOs	0.32	0.31	0.19	0.51	0.45	0.47	0.36	0.53	0.49	0.36	–	–	0.19	0.12	0.14	0.03	0.21	0.16	0.04	–	–	57%	37%	43%	11%	64%	51%	12%
Mean Length of HARFOs	0.97	0.96	0.98	0.98	0.79	0.94	0.88	0.96	0.96	0.95	–	0.01	0.01	–	–	–	–	–	–	–	1%	1%	–	–	–	–	–	–
Mean Aspect Ratio of WHOFOs	0.29	0.39	0.36	0.41	0.33	0.39	0.32	0.21	0.23	0.60	0.09	0.07	0.12	0.04	0.10	0.03	–	–	0.30	32%	25%	40%	14%	34%	9%	–	–	105%
Mean Aspect Ratio of HARFOs	0.58	0.66	0.70	0.51	0.78	0.76	0.68	0.36	0.44	0.88	0.08	0.12	–	0.20	0.18	0.10	–	–	0.30	14%	21%	–	35%	31%	17%	–	–	51%
Mean Diameter of WHOFOs	0.98	0.96	0.96	1.00	0.91	1.00	0.85	0.99	0.94	0.92	–	–	0.02	–	0.02	–	–	–	–	–	–	2%	–	2%	–	–	–	–
Mean Diameter of HARFOs	0.91	0.90	0.98	0.91	0.82	0.76	0.83	0.97	0.96	0.96	–	0.07	–	–	–	–	0.06	0.05	0.05	–	8%	–	–	–	–	6%	5%	5%
WHOFOs to HARFOs	0.63	0.80	0.76	0.88	0.89	0.55	0.78	0.48	0.48	0.64	0.17	0.13	0.26	0.26	–	0.16	–	–	0.01	27%	21%	41%	41%	–	25%	–	–	2%